Original Article
Food Science and Technology

ISSN 0101-2061 (Print)
ISSN 1678-457X (Online)

DOI: https://doi.org/10.1590/fst.96722

Study on the detection of apple soluble solids based on fractal theory and hyperspectral imaging technology

Xueting MA[1,2], Huaping LUO[1,2*], Jiean LIAO[1,2], Lixia ZHU[3*], Jinfei ZHAO[1,2], Feng GAO[1,2]

Abstract

To explore a new method for the detection of soluble solids content (SSC) in apples, the reflectance spectra of apples with different SSC were obtained based on hyperspectral imaging technology in this paper, and fractal measurement of the reflection spectrum curve was carried out based on fractal theory, for using fractal dimension to quantitatively reflect its SSC. The results show that the samples with different SSC have little difference in fractal dimension, and are not sensitive to the change of apple SSC, which cannot show an obvious linear relationship. It can be considered to conduct a study on discrimination with obvious differences between spectral curves, such as variety discrimination and damage discrimination.

Keywords: apple; hyperspectral imaging; fractal theory; fractal dimension; SSC.

Practical Application: A new parameter for fruit quality description, namely fractal dimension, is proposed, which provides a certain reference for the application of this method in fruit quality evaluation.

1 Introduction

Soluble solid content (SSC) is an important component that determines apple taste and quality (Biegert et al., 2021). Accurate estimation of SSC is of great significance for research and application of apple quality evaluation (Tian et al., 2022). Spectral technology provides an important method for nondestructive testing of soluble solid content. At present, the research of fruit internal and external quality detection based on spectral technology has become one of the important research directions of many scholars. Gao & Wang (2021) studied a non-destructive detection method of glucose content and water content in the grape based on visible/near-infrared spectral transmission technology. By collecting 360 red globe grape samples, the partial least-square regression (PLSR) and Least Squares SVM (LSSVM) detection models of glucose content and water content in the red globe were established respectively. The results show that the non-destructive detection method of glucose and moisture in red earth based on visible light/near-infrared technology is feasible, and the detection accuracy of the two optimal detection models can meet the detection requirements. Qi et al. (2022) classified the near-infrared spectra of red jujube samples based on the near-infrared spectroscopy technology and a fuzzy improved linear discriminant analysis (FILDA) algorithm to identify the red jujube varieties quickly, losslessly and effectively. The classification accuracy was 94.4%. These results showed that FILDA combined with near infrared spectroscopy was an effective method for the identification of red jujube varieties and had a broad application prospect. Yuan et al. (2022) obtained the reflectance (R), absorbance (a) and Kubelka Munk (K-M) spectra of jujube through the hyperspectral imaging system and applied them to non-destructive detection of bruise symptoms. Partial least squares discriminant analysis (PLS-DA) and support vector machine (SVM) were used to establish the classification and discrimination model. The results show that PLS-DA model has the lowest error in cross validation, while the number of characteristic variables is the lowest, accounting for 28.8%. The accuracy of calibration and cross validation are 88.9% and 100.0%, respectively. At present, most of the inputs of the prediction models studied are characteristic bands, while the methods of quantitative description (or measurement) of characteristic bands are less studied in the field of fruit detection.

The fractal theory is a science that studies a kind of irregular, chaotic and complex system with local and global similarities (Zhao et al., 2022). Fractal dimension is a basic measure used to describe the irregularity and self-similarity of objects in fractal theory (Acquisgrana et al., 2022; Han et al., 2022). In this paper, fractal dimension is proposed as a method to identify spectral characteristics to explore the relationship between fractal dimension and soluble solid content (SSC). Firstly, the apple spectral signal is obtained based on hyperspectral imaging technology, and the characteristic band is selected. Then, the fractal dimension of the characteristic spectrum signal is calculated based on the compass fractal dimension calculation method. By comparing the fractal dimension of the apple spectrum signal with different SSC, the relationship between the fractal dimension and SSC is explored, to provide a new idea of quantitatively reflecting SSC of the apple with the fractal dimension.

Received 06 Aug., 2022
Accepted 13 Oct., 2022
[1] *Modern Agricultural Engineering Key Laboratory at Universities of Education Department of Xinjiang Uygur Autonomous Region, Tarim University, Alar, China*
[2] *College of Mechanical and Electrical Engineering, Tarim University, Alar, China*
[3] *College of Food Science and Engineering, Tarim University, Alar, China*
*Corresponding author: hpluo739@163.com; 120050068@taru.edu.cn

2 Materials and methods

2.1 Sample collection

Fuji Apple was selected as the research object. The sample was collected from Hongqipo farm in Aksu, Xinjiang, China in late October 2021. The region belongs to a temperate continental climate, with a long illumination time and a large temperature difference between day and night. The annual average temperature is 9.9 °C ~ 11.5 °C, and the annual frost-free period is 183 ~ 228 days. We selected 60 apples of uniform size and washed the collected apples with clean water. After that, we placed them in the laboratory to dry, and then number the samples separately.

2.2 Apple hyperspectral data acquisition and processing

Hyperspectral detection system and parameter setting

The hyperspectral imaging system is shown in Figure 1, which is composed of an imaging spectrometer (image- λ - N17E, Sichuan Shuangli Hepu Technology Co., Ltd.), a tungsten halogen lamp with stable power (140 W), a set of high-precision electronic control mobile platform and a computer. To reduce the influence of ambient light on image acquisition, the image acquisition system was placed in a dark box (65 cm × 50 cm × 110 cm). The hyperspectral camera has a spectral range of 900~1750 nm, 254 bands, a spectral resolution of 5 nm, and an incident light slit width of 30 μm.

Before acquiring hyperspectral images, we first set its object distance (45 cm) and exposure time (11.5 ms). The hyperspectral imaging system relies on the mobile platform to complete the push scan acquisition of images. To get a clear image, the speed of the mobile platform should not be too high. Through experiments, when the platform runs at the speed of 2.0 m/min, the effect is good.

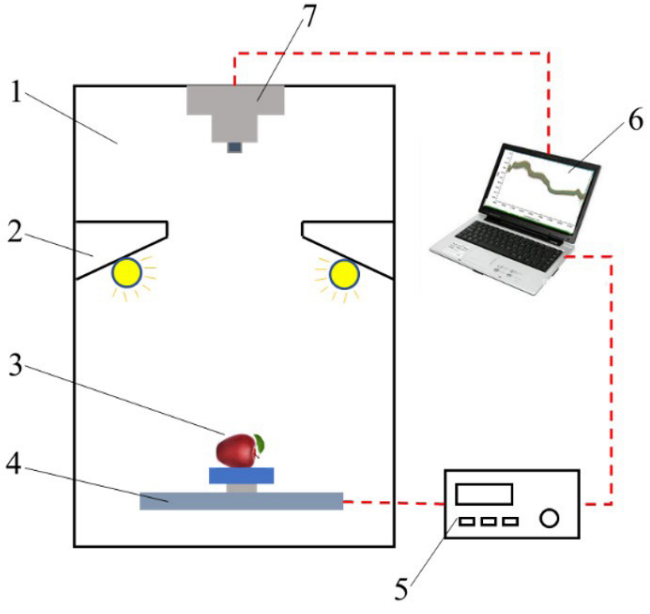

Figure 1. Schematic diagram of the hyperspectral imaging system. 1. Dark box. 2. Light source. 3. Sample. 4. Mobile platform. 5. Platform controller. 6. Computer. 7. Spectral camera.

Black and white plate correction of hyperspectral images

When collecting hyperspectral images in the dark box, the hyperspectral images will still contain a lot of noise due to the power stability of CCD cameras, the nonuniformity of the light source in some bands, and the diffuse reflection of the fruit surface on the light source, although the influence of natural light is excluded (Jiang et al., 2022). We choose to use black and white plate correction to reduce the influence to achieve reflectivity calibration of hyperspectral images. We first cover the lens with the lens cover to acquire the dark background image D, then take down the lens, place the whiteboard to make the height of the whiteboard consistent with the height of the apple sample, and acquire the whiteboard hyperspectral image W. The correction algorithm is as follows (Jiang et al., 2022; Zou et al., 2022) (Equation 1):

$$R = \frac{(S - D)}{(W - D)} \quad (1)$$

Where R is the corrected image data, S is the original hyperspectral image data of the sample, and W is the whiteboard calibration data. D is dark background calibration data.

2.3 Apple soluble solid content acquisition

The apple SSC was measured by a hand-held Brix meter (GMK-701R, G-won company, South Korea), with a measurement range of 0 ~ 45 ° Brix and a resolution of 0.1 ° Brix. When measuring the SSC of the sample, the pulp was taken out at a 6 mm depth from the part where the spectrum was collected, the pulp was squeezed and the juice was dropped on the detection window of the Brix meter. The average value of three repeated collections was taken as the true value. The SSC of the tested sample set is between 14.2 and 19.9 ° Brix, with a total of 60 samples.

2.4 Fractal theory and fractal dimension calculation method of apple spectral curve

Fractal theory researchers have given different definitions of fractal in different periods, but so far there is no exact and unified definition. Generally, fractals are regarded as a set F with the following typical properties.

(1) F has a fine structure, that is, details of arbitrarily small scale;

(2) F is so irregular that neither its parts nor its whole can be described in traditional geometric language;

(3) F usually has some kind of self-similar form;

(4) In most cases, F can be defined in a very simple way and can be generated by iteration.

Generally, the object can be considered to have fractal characteristics, if the studied object satisfies all or most of the above properties.

Fractal dimension is a basic measure used to describe the irregularity and self-similarity of objects in fractal theory. In this

paper, fractal dimension is used to describe the irregularity of the spectral curve. The commonly used methods for calculating fractal dimension include the box method (Gao et al., 2021), and the variance method (Pouraimis et al., 2021). Since the local variation of the reflection spectrum curve will affect the whole curve, this paper uses a compass dimension that can effectively reduce the impact of the local variation on the whole curve (Cao et al., 2021).

The compass dimension algorithm can obtain the fractal dimension of the spectral reflection curve by changing the scale of the circle. The solving process of compass dimension includes three steps: spectral curve preprocessing, iterative calculation and linear fitting.

(1) Envi 5.1 (Research System Inc, Boulder, Co., USA) was used to extract the average spectral curve of the circular ROI with a radius of 25 pixels in the acquired hyperspectral image, and the continuum removal was performed (Bai et al., 2022; Guo et al., 2021). Considering the systematic error and saturation phenomenon, it is necessary to select a suitable band during spectral analysis, and use Savitzky-Golay (S-G) filtering method to smooth the average spectral reflection curve to obtain a smooth spectral reflection curve.

(2) Iterative calculation. After the average spectral curve of each ROI is processed by S-G, a smooth spectral curve is obtained, and then we solve the fractal dimension. The solution flow chart is shown in Figure 2.

(3) The fractal dimension D_i is calculated according to Equation 2.

$$D_i = -\frac{\lg T(r_i)}{\lg \frac{1}{r_i}} \left(i = 1, 2, \cdots, M\right) \quad (2)$$

Where, D_i is the compass dimension value of the reflection spectrum curve, and its value is between 1 and 2. Figure 3 shows the calculation process of the compass dimension of a certain spectral curve of apple.

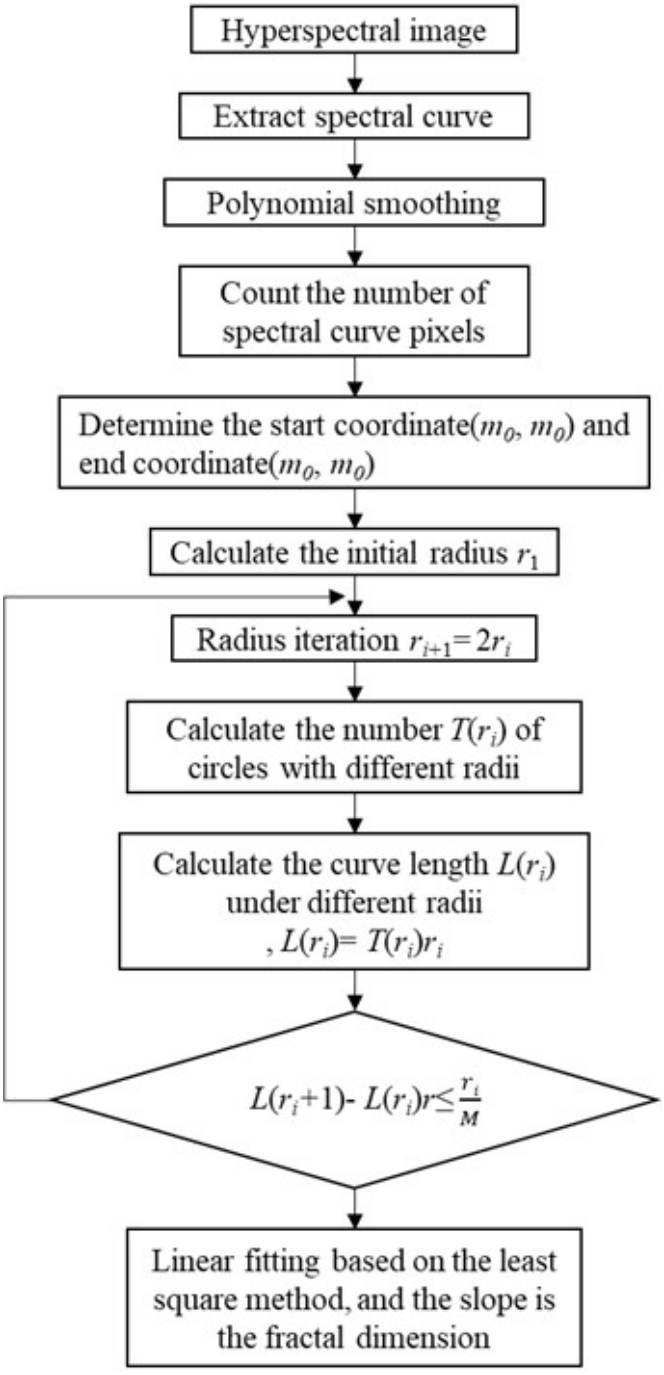

Figure 2. Calculation process of fractal dimension.

3 Results and discussion

3.1 Apple spectrum pretreatment analysis

Hyperspectral data were collected from apple samples with different SSC. After the collection, ENVI software was used to select a circular region with a radius of 25 pixels as ROI, and the average spectral curve of each apple was obtained (Yang et al., 2022), and the spectral curve was processed by the continuum removal (Figure 4).

It can be seen from Figure 3 that the spectrum curves of apples with different SSC have the same trend in the range of 900~1750 nm, and the curves under some bands overlap, making it difficult to identify the difference between the spectra. We can see that there are troughs at 1450 nm, 1200 nm, 1000 nm and 930 nm, and peaks at 1660 nm, 1270 nm and 950 nm. In the range of 1050 ~ 1150 nm and 900 ~ 950 nm, the curves overlap seriously, while the spectral curves in the range of 1150 ~ 1650 nm have obvious differences.

To combine more spectral information and take into account the systematic error and saturation phenomenon, a total of 191 bands between 1100 and 1650 nm are selected. The average spectral reflection curve is smoothed by Savitsky-Golay (S-G) filtering method to obtain a smooth spectral reflection curve, as shown in Figure 5.

3.2 Calculation results of fractal dimension

We calculated the fractal dimension of the spectral curves of 60 apple samples (see Table 1). The results show that the fractal dimension of the 60 spectra has little difference between the maximum and minimum values, which are 1.0407 and 1.0454, respectively; the standard deviation is 0.0012, indicating that the fractal dimension of 60 samples fluctuates less. The distribution range and fluctuation of fractal dimension are both small, which is not conducive to the quantitative description of apple's physical and chemical indicators based on this parameter.

Figure 6 is a scatter plot of the relationship between fractal dimension and apple SSC. As can be seen from the figure, there is no obvious correlation between the two. This may be related to the small difference in the fractal dimension of apples with different SSC, or it may be related to the fact that the obtained spectrum is a reflection spectrum (the quantitative detection effect of the transmission spectrum is better for the internal quality of the fruit).

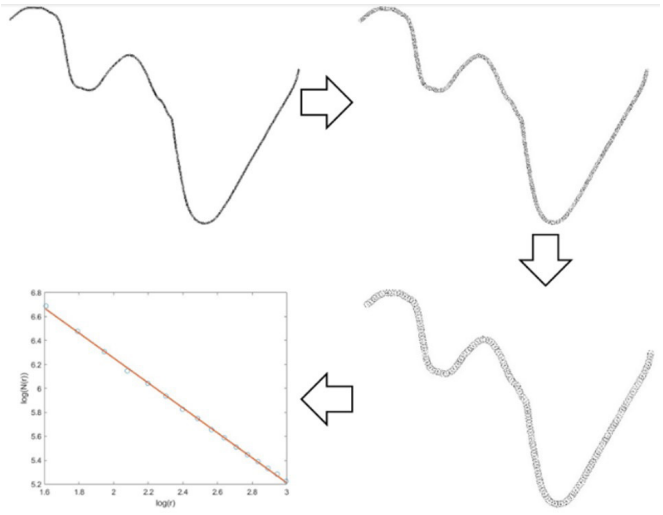

Figure 3. Dimension calculation of spectrum.

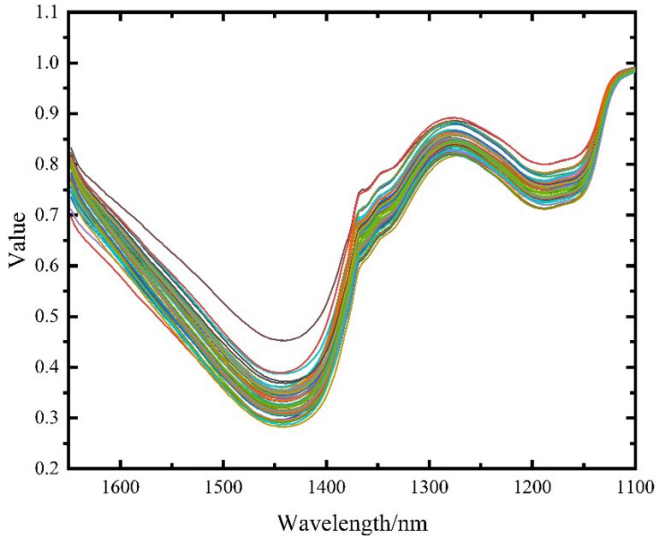

Figure 5. Spectrum after pretreatment.

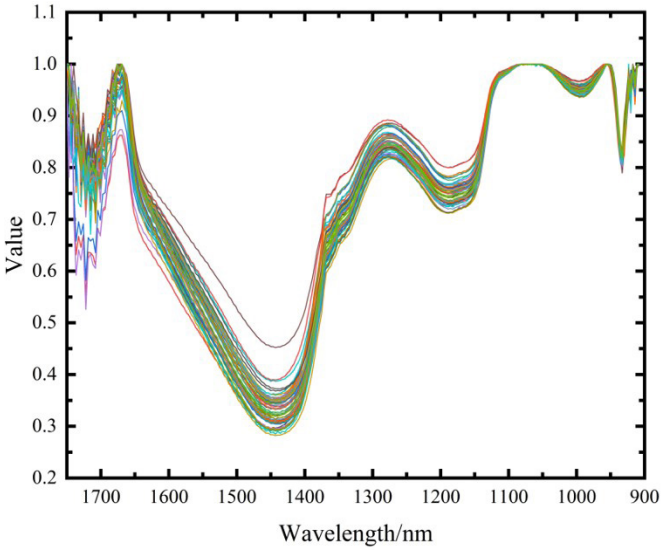

Figure 4. Spectral curve after continuum removal.

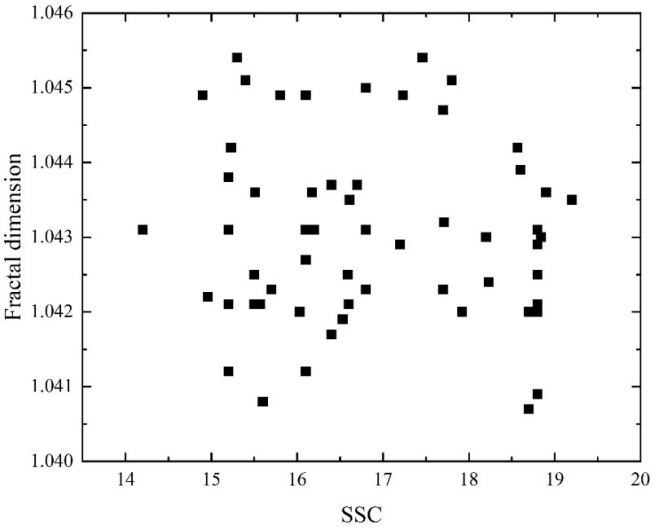

Figure 6. Scatter plot of fractal dimension and SSC.

Table 1. Fractal dimension calculation results.

Number of samples	Maximum value	Minimum	Average value	Standard deviation
60	1.0454	1.0407	1.0428	0.0012

4 Conclusion

This paper proposes a method to quantitatively describe apple SSC based on fractal dimension. The hyperspectral curve and SSC of the sample were obtained separately, and the corresponding relationship between the two was tried to be established. However, the results show that the distribution range of the sample fractal dimension is narrow, the data volatility is small, and there is no correlation with apple SSC. In the follow-up research, we can consider the study on the discrimination between the obvious shapes of apples (such as apple variety discrimination, damage discrimination and mildew discrimination) based on fractal theory, which may be more effective in discriminating between significantly different spectra.

Ethical approval

This article does not contain any studies with human participants or animals performed by any of the authors.

Conflict of interest

The authors declare no conflict of interest.

Availability of data and material

All data are available from the corresponding author.

Funding

This project was supported by the Key scientific and technological projects of Xinjiang Construction Corps (2018AB042), the National Natural Science Foundation of China (11964030); the Open Project of Key Laboratory of Modern Agricultural Engineering in Colleges and Universities of the Department of Education of the Autonomous Region (TDNG2021201).

References

Acquisgrana, M. R., Pamies, L. C. G., Quiroga, F., Ribotta, P. D., & Benítez, E. I. (2022). Impact of sorghum grain processing on morphological characteristics of particles of wholegrain sorghum flour. *Food Science and Technology*, 42, e69420. http://dx.doi.org/10.1590/fst.69420.

Bai, H., Yang, Y., Cui, Q., Jia, P., & Wang, L. (2022). Retrieval of heavy metal content in soil using GF-5 satellite images based on GA-XGBoost model. *Jiguang Yu Guangdianzixue Jinzhan*, 59(12), 1230001.

Biegert, K., Stockeler, D., McCormick, R. J., & Braun, P. (2021). Modelling soluble solids content accumulation in 'Braeburn' apples. *Plants*, 10(2), 302. http://dx.doi.org/10.3390/plants10020302. PMid:33562496.

Cao, Y., Yuan, P., Wang, H., Tchalla, W. K., Fan, J., & Xu, H. (2021). Monitoring index of rice bacterial blight based on hyperspectral fractal dimension. *Nongye Jixie Xuebao*, 52(9), 134-140.

Gao, H. B., Liang, Y. S., & Xiao, W. (2021). Relationship between upper box dimension of continuous functions and orders of weyl fractional integral. *Fractals*, 29(7), 2150223. http://dx.doi.org/10.1142/S0218348X21502236.

Gao, S., & Wang, Q.-H. (2021). Non-destructive testing of red globe grape sugar content and moisture content based on visible/near infrared spectroscopy transmission technology. *Chinese Optics*, 14(3), 566-577. http://dx.doi.org/10.37188/CO.2020-0085.

Guo, J., Zhang, J., Xiong, S., Zhang, Z., Wei, Q., Zhang, W., Feng, W., & Ma, X. (2021). Hyperspectral assessment of leaf nitrogen accumulation for winter wheat using different regression modeling. *Precision Agriculture*, 22(5), 1634-1658. http://dx.doi.org/10.1007/s11119-021-09804-z.

Han, H. X., Ma, Y., He, W., Yang, W. F., & Fu, X. D. (2022). Numerical simulation of rockfill materials based on fractal theory. *Applied Sciences*, 12(1), 289. http://dx.doi.org/10.3390/app12010289.

Jiang, R.-C., Gu, M.-S., Zhao, Q.-H., Li, X.-R., Shen, J.-X., & Su, Z.-B. (2022). Identification of pesticide residue types in Chinese cabbage based on hyperspectral and convolutional neural network. *Guangpuxue Yu Guangpu Fenxi*, 42(5), 1385-1392.

Pouraimis, G., Kotopoulis, A., Massinas, B., & Frangos, P. (2021). Sea state characterization using experimental one-dimensional radar signatures and fractal techniques. *Elektronika ir Elektrotechnika*, 27(3), 71-77. http://dx.doi.org/10.5755/j02.eie.28906.

Qi, Z., Wu, X., Yang, Y., Wu, B., & Fu, H. (2022). Discrimination of the red jujube varieties using a portable NIR spectrometer and fuzzy improved linear discriminant analysis. *Foods*, 11(5), 763. http://dx.doi.org/10.3390/foods11050763. PMid:35267396.

Tian, Y., Sun, J., Zhou, X., Yao, K. S., & Tang, N. Q. (2022). Detection of soluble solid content in apples based on hyperspectral technology combined with deep learning algorithm. *Journal of Food Processing and Preservation*, 46(4), e16414. http://dx.doi.org/10.1111/jfpp.16414.

Yang, S., Zhang, H. Q., & Fan, W. M. (2022). Characteristic wavelengths selection of rice spectrum based on adaptive sliding window permutation entropy. *Food Science and Technology*, 42, e38922. http://dx.doi.org/10.1590/fst.38922.

Yuan, R. R., Guo, M., Li, C. Y., Chen, S. T., Liu, G. S., He, J. G., Wan, G. L., & Fan, N. Y. (2022). Detection of early bruises in jujubes based on reflectance, absorbance and Kubelka-Munk spectral data. *Postharvest Biology and Technology*, 185, 111810. http://dx.doi.org/10.1016/j.postharvbio.2021.111810.

Zhao, F. W., Hu, J. H., Yang, Y. A., Xiao, H. X., & Ma, F. C. (2022). Cross-scale study on lime modified phosphogypsum cemented backfill by fractal theory. *Minerals*, 12(4), 403. http://dx.doi.org/10.3390/min12040403.

Zou, Z. Y., Wu, Q. S., Chen, J., Long, T., Wang, J., Zhou, M., Zhao, Y. P., Yu, T. J., Wang, Y. F., & Xu, L. J. (2022). Rapid determination of water content in potato tubers based on hyperspectral images and machine learning algorithms. *Food Science and Technology*, 42, e46522. http://dx.doi.org/10.1590/fst.46522.